

Enhanced ponderomotive force in graphene due to interband resonance

C. Wolff,^{1,*} C. Tserkezis,¹ and N. Asger Mortensen^{1,2,3}

¹*Center for Nano Optics, University of Southern Denmark, Campusvej 55, DK-5230 Odense M, Denmark*

²*Danish Institute for Advanced Study, University of Southern Denmark, Campusvej 55, DK-5230 Odense M, Denmark*

³*Center for Nanostructured Graphene, Technical University of Denmark, DK-2800 Kongens Lyngby, Denmark*

(Dated: January 28, 2019)

We analyze intrinsic nonlinearities in two-dimensional polaritonic materials interacting with an optical wave. Focusing on the case of graphene, we show that the second-order nonlinear optical conductivity due to carrier density fluctuations associated with the excitation of a plasmon polariton is closely related to the ponderomotive force due to the oscillating optical field. This relation is first established through an elegant thermodynamic approach for a Drude-like plasma, in the frequency range where intraband scattering is the dominant contribution to conductivity. Subsequently, we extend our analysis to the interband regime, and show that for energies approximately half the Fermi energy, the intraband contribution to the ponderomotive force diverges. In practice, thermal broadening regularizes this divergence as one would expect, but even at room temperature typically leaves a strong ponderomotive enhancement. Finally, we study the impact of nonlocal corrections and find that nonlocality does not lead to further broadening (as one would expect in the case of Landau damping), but rather to a splitting of the ponderomotive interband resonance. Our analysis should prove useful to the open quest for exploiting nonlinearities in graphene and other two-dimensional polaritonic materials, through effects such as second harmonic generation and photon drag.

I. INTRODUCTION

The emergence of graphene [1, 2] and other two-dimensional (2D) materials [3, 4] at the forefront of research in all areas of condensed matter physics, owing to their intriguing mechanical [5], thermal [6], electronic [7] and optical properties [8], has led to a plethora of suggested applications, many of which are already starting to see the light of day. In photonics, in particular, where the possibility to excite and tailor highly confined polaritons can have important implications [9, 10], 2D materials became very quickly prominent templates for enabling and tailoring light-matter interactions [11–13]. In this context, the prospect of enhanced nonlinearities is always among the first effects to be explored in a novel architecture, and 2D materials could not fail to attract their share of attention [14–18].

In the long list of nonlinear optical effects, such as higher-harmonic generation, stimulated Raman and Rayleigh scattering, electrooptic effects and multiphoton absorption [19], ponderomotive effects are particularly relevant to plasmonics. Charged particles in inhomogeneous oscillating electromagnetic fields are known to be subject to a ponderomotive force proportional to the gradient of the electric field ($\vec{F} \propto \text{grad}|\vec{E}|^2$) that accelerates them towards the field direction [20]. This has been exploited, for instance, for electron acceleration with laser pulses [21], and controlling excitons [22] or plasmons [23], as well as inducing nonlinear effects in them [24, 25]. With the advent of graphene as an exemplary plasmonic medium, it was only natural to explore its capability to enhance nonlinearities [26–28], and

the ponderomotive force can be a mechanism to lead to, otherwise symmetry-prohibited, second harmonic generation (SHG) [15].

Recently, the second-order nonlinear ac conductivity of a generic Dirac fluid was connected to the ponderomotive force through the hydrodynamic equations of motion [29]. As a directly available test bed, the authors of Ref. 29 applied their analysis to graphene, focusing on SHG and photon drag. While they limited themselves to the energy regime dominated by intraband transitions, they anticipated that at high (e.g. room) temperatures the interband contribution to the conductivity could become important. This is exactly the focus of this paper. We start by deriving the connection between the ac conductivity and the ponderomotive force with a different starting point, through a general and powerful thermodynamic approach which, to the best of our knowledge, has not been presented before. By introducing the second-order, room-temperature expression for the conductivity of graphene, we show that the resulting ponderomotive force exhibits a resonance at an energy twice the Fermi energy, becoming infinite at zero temperature. This resonant behavior survives for higher temperatures, and can lead to forces as large as one order of magnitude stronger than in the intraband case, over a relatively wide energy range.

II. PRELIMINARIES

We consider a graphene monolayer sandwiched between two dielectrics with relative permittivities ϵ_1 and ϵ_2 . Within a local response approximation, the electromagnetic properties of graphene are characterized by a complex sheet conductance $\sigma(\omega)$. It has two contribu-

* cwo@mci.sdu.dk

tions ($\sigma = \sigma_1 + \sigma_2$): firstly a Drude model

$$\frac{\sigma_1(\omega)}{\sigma_K} = \frac{i2\mathcal{E}_F}{\hbar(\omega + i\gamma)}, \quad (1a)$$

due to intraband scattering of free carriers. It is characterized by a Ohmic damping constant γ due to the scattering of carriers predominantly off lattice impurities at low temperatures and phonons at higher temperatures. The second contribution describes the effect of interband transitions if the photon energy $\hbar\omega$ exceeds twice the Fermi energy \mathcal{E}_F (relative to the undoped state). At zero

temperature. it takes the form:

$$\frac{\sigma_2^{(T=0)}(\omega)}{\sigma_K} = \frac{\pi}{2} \left(\Theta(\hbar\omega - 2\mathcal{E}_F) + \frac{i}{\pi} \ln \left| \frac{\hbar\omega - 2\mathcal{E}_F}{\hbar\omega + 2\mathcal{E}_F} \right| \right). \quad (1b)$$

Here, \hbar is Planck's constant, $\Theta(x)$ is the Heaviside function, and $\sigma_K = e^2/h \simeq 0.387 \times 10^{-5} \text{ S}$ is the inverse of the von-Klitzing constant, with e being the electron charge [11].

The full optical conductivity of graphene at finite temperature has been calculated in Refs. 30 and 31

$$\frac{\sigma^{(T>0)}(\omega)}{\sigma_K} = \frac{i2\mathcal{E}_F}{\hbar(\omega + i\gamma)} + \frac{\pi}{4} \left(\tanh \frac{\hbar\omega + 2\mathcal{E}_F}{4k_B T} + \tanh \frac{\hbar\omega - 2\mathcal{E}_F}{4k_B T} + \frac{i}{\pi} \ln \frac{(\hbar\omega - 2\mathcal{E}_F)^2 + (2k_B T)^2}{(\hbar\omega + 2\mathcal{E}_F)^2} \right), \quad (2)$$

where k_B is the Boltzmann constant and T the temperature. This expression can be further corrected through appropriate multiplicative factors proportional to the square of the energy over the hopping parameter of the tight-binding description of graphene [30]. However, this correction is usually of minor importance [26, 31], and our calculations showed that it can be safely disregarded here as well.

Graphene is best known and has received most of its attention because of its linear energy-momentum relation at the undoped Fermi energy [11]. This implies that the common expression $m_{\text{eff}} = \hbar^2 [\partial^2 \mathcal{E} / \partial k^2]^{-1}$ for the electron effective mass is ill-defined for its quasiparticles, which in fact have vanishing “rest mass”. Instead, the appropriate expression for the effective mass is the dynamic mass of a relativistic massless particle, where the energy-independent Fermi velocity v_F takes the role of the speed of light [1]:

$$\mathcal{E} = m_{\text{eff}} v_F^2. \quad (3)$$

In further analogy to relativistic massless particles, the Fermi wave number q_F is related to the Fermi energy via the linear relationship

$$\mathcal{E}_F = \hbar v_F q_F. \quad (4)$$

Finally, the Fermi wave number is directly connected to the density n of free carriers:

$$q_F = \sqrt{\pi n}. \quad (5)$$

Here, we study how a plasmon polariton and an optical wave interact in a graphene sheet due to the intrinsic nonlinearity of graphene. To this end, we introduce a separation of scales. The optical wave is assumed to oscillate at an angular frequency ω , whereas the polariton oscillates at an angular frequency $\Omega \ll \omega$. As a result,

the optical parameters can be assumed to be modified by the polariton, but remain quasi-stationary as far as the optical wave is concerned. This separation of frequency scales is intrinsic to the notion of the ponderomotive force. Finally, our thermodynamic argument assumes a macrocanonical ensemble characterized by the free enthalpy \mathcal{G} .

III. INTRABAND CONTRIBUTION TO NONLINEAR RESPONSE

First, we derive the ponderomotive force ignoring interband transitions. The basic idea is that a plasmon polariton is in essence a fluctuation in the carrier density, and therefore accompanied by a spatial modulation of the local Fermi level \mathcal{E}_F . The notion of a local Fermi level is acceptable as long as the polaritonic wavelength is much larger than the lattice constant of the graphene molecule, i.e. whenever local response theory applies. It also implies the assumption that the polariton does not cause too much “unrest” in the electron system, but rather moves carriers around in a quasi-adiabatic way while overall maintaining the general shape of the Fermi distribution. This can be expected whenever the polariton experiences low loss, as any qualitative distortion of the Fermi distribution really means dissipation. The Fermi level in turn controls the intraband conductance of graphene through Eq. (1a) and is linked to the total carrier density through Eq. (5). This means that we can estimate the change to the optical response simply through the chain rule:

$$\frac{\partial \sigma_1}{\partial n} = \frac{\partial \sigma_1}{\partial \mathcal{E}_F} \frac{\partial \mathcal{E}_F}{\partial n} = \frac{ie^2 v_F}{2\hbar(\omega + i\gamma)\sqrt{\pi n}} = \frac{\sigma_1}{2n}. \quad (6)$$

We now aim to gain a better understanding of the expression Eq. (6) for the polariton-induced change to

the optical properties. To this end, we recall the definition of a permittivity from the total free enthalpy $\tilde{\mathcal{G}}$ of a solid [20]:

$$[\varepsilon_r]_{ij} = -\frac{1}{\varepsilon_0} \cdot \frac{\partial^2 \tilde{\mathcal{G}}}{(\partial E_i)(\partial E_j)}. \quad (7)$$

Using the relationship $\sigma = -i\omega\varepsilon_0\varepsilon_r$ between the complex conductance and the permittivity of a material, we can adapt Eq. (7) to the case of an isotropic sheet conductance:

$$\sigma = i\omega \frac{\partial^2 \tilde{\mathcal{G}}}{\partial |\vec{E}_{\parallel}|^2}, \quad (8)$$

where \vec{E}_{\parallel} is the tangential field at the position of the sheet. The fact that \vec{E}_{\parallel} is continuous across the sheet motivates why \vec{E} was chosen as the independent variable [32] in Eq. (7).

Using Eq. (8), we can characterize the intrinsic second-order nonlinearity of graphene by a parameter W via:

$$W = \frac{\partial}{\partial n} \left[\frac{\partial^2 \tilde{\mathcal{G}}}{\partial |\vec{E}_{\parallel}|^2} \right] = \frac{\sigma_1}{2in\omega}. \quad (9)$$

Under the assumption that this nonlinear process in itself is reversible, we can interchange the order of derivatives and also find

$$W = \frac{\partial^2}{\partial |\vec{E}_{\parallel}|^2} \left[\frac{\partial \tilde{\mathcal{G}}}{\partial n} \right]. \quad (10)$$

This time, the term in brackets is the definition of a local chemical potential, so Eq. (10) describes a correction to the chemical potential caused by a change in the intensity of a quickly oscillating electric field. This is of course just a Maxwell relation and intimately related to the Manley–Rowe relations known from nonlinear optics and electrical engineering [19]. Even though it sounds similar to our starting point (change of the Fermi level due to a propagating polariton), it describes in fact the inverse process. Again, it should be stressed that this conclusion requires the nonlinear interaction to be reversible, i. e. not to create any entropy, not to be dissipative. Therefore, we can expect this to hold exactly in the limit $\gamma = 0$ and gradually be broken as γ assumes a finite value.

From Eq. (6), we can see that W does not depend on the electric field, so we can derive from Eq. (10) an explicit expression for the change in chemical potential

$$\Delta\mu = \frac{\partial \tilde{\mathcal{G}}}{\partial n} = W |\vec{E}_{\parallel}|^2. \quad (11)$$

This exerts a force on each particle that is proportional to the in-plane gradient:

$$\vec{F}_1 = \text{grad}_{\parallel}(\Delta\mu) = \frac{\sigma_1}{2in\omega} \text{grad}_{\parallel} |\vec{E}_{\parallel}|^2, \quad (12)$$

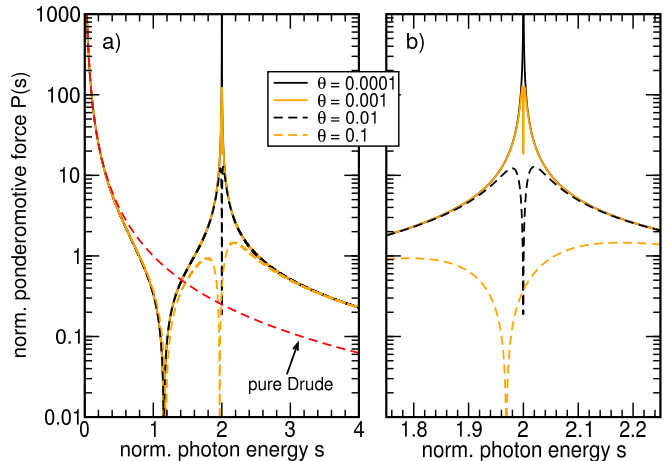


FIG. 1. Dependence (overview in panel a, close-up of the interband resonance in panel b) of the frequency-part $P(s)$ of the finite-temperature ponderomotive force as defined in Eq. (17) on the normalized photon energy $s = \hbar\omega/\mathcal{E}_F$ for the annotated values of the normalized temperature $\theta = k_B T/\mathcal{E}_F$. For $\mathcal{E}_F = 893$ meV, the temperatures correspond to 1, 10, 100, and 1000 K, respectively. The red dashed line indicates the pure Drude-like ponderomotive force without interband contributions for comparison.

where grad_{\parallel} represents the 2D gradient operator in the sheet plane. Finally, in the limit of vanishing loss ($\gamma \rightarrow 0$) and using Eqs. (3–5), we find:

$$\vec{F} = \frac{e^2}{2m_{\text{eff}}\omega^2} \text{grad}_{\parallel} |\vec{E}_{\parallel}|^2. \quad (13)$$

This is the expression for the ponderomotive force in a 2D plasma composed of particles with effective mass m_{eff} . Therefore, we have established that the intrinsic nonlinear change of the optical conductance due to a plasmon polariton in a graphene sheet is the complementary process to the ponderomotive force through which variations in the intensity of an optical field can drive polaritons.

A similar expression was recently derived in Ref. 29, albeit with a different starting point and analysis, and restricted to the intraband scattering region. Nevertheless, the authors of Ref. 29 did stress the necessity to explore interband corrections, already proven to be capable of enhancing third-order nonlinearities [33] or contributing to difference frequency generation [34], and this is what we shall do in the next section.

IV. INTERBAND CONTRIBUTION

The connection we established in the previous section now allows us to find the generalized ponderomotive force in situations where the electron system can no longer be described as a Drude plasma. This is for example the case in the regime $2\hbar\omega \gtrsim \mathcal{E}_F$, where the electromagnetic response is significantly modified by interband transitions.

Following our previous analysis, we can express the correction to the ponderomotive force in terms of the density derivative of the interband conductance, provided this nonlinear coefficient describes a reversible process. For optical frequencies $\omega \neq 2\mathcal{E}_F/\hbar$, we find:

$$\vec{F}_2^{(T=0)} = \frac{1}{i\omega} \cdot \frac{\partial \sigma_2^{(T=0)}}{\partial n} \text{grad}_{\parallel} |\vec{E}_{\parallel}|^2 \quad (14a)$$

$$= \frac{\hbar e^2 v_F^2}{8\mathcal{E}_F^2 - 2(\hbar\omega)^2} \text{grad}_{\parallel} |\vec{E}_{\parallel}|^2. \quad (14b)$$

This expression is purely real-valued, i. e. the variation in the Fermi level does not lead to a change in the ab-

sorptivity of the material unless the optical frequency is chosen such that $\hbar\omega - 2\mathcal{E}_F$ changes sign. Only in this case, the nonlinearity features a substantial imaginary part, i. e. becomes dissipative. Otherwise, Eq. (14b) constitutes a real ponderomotive force. Due to the resonant nature of Eq. (14b), this force diverges as the optical frequency approaches the interband threshold from either side, especially from the low-loss side. In theory, the ponderomotive forces per unit of optical intensity can be made arbitrarily large by moving towards the point $\omega = 2\mathcal{E}_F/\hbar$. This divergence is of course just an artifact of assuming the step-like Fermi distribution at zero temperature and will be regularized for any $T \neq 0$.

Indeed, starting from Eq. (2), we find that the real pole turns into a Lorentzian imaginary part:

$$\frac{1}{\sigma_K} \frac{\partial \sigma_2^{(T>0)}}{\partial \mathcal{E}_F} = \frac{\pi}{8k_B T} \left[\text{sech}^2 \frac{\hbar\omega + 2\mathcal{E}_F}{4k_B T} - \text{sech}^2 \frac{\hbar\omega - 2\mathcal{E}_F}{4k_B T} \right] + \frac{i}{\hbar\omega + 2\mathcal{E}_F} + \frac{i(\hbar\omega - 2\mathcal{E}_F)}{(\hbar\omega - 2\mathcal{E}_F)^2 + (2k_B T)^2}. \quad (15)$$

Due to the more broadband loss of interband transitions at finite temperature, this derivative is non-real everywhere, so strictly speaking, it does not provide a real ponderomotive force. However, at least in parameter ranges where the real part of Eq. (15) is small, we can regard inserting its imaginary part in Eq. (14a) to be a good approximation:

$$\vec{F}_2^{(T>0)} \approx \frac{\hbar e^2}{4\omega m_{\text{eff}}} \left[\frac{\hbar\omega - 2\mathcal{E}_F}{(\hbar\omega - 2\mathcal{E}_F)^2 + (2k_B T)^2} + \frac{1}{\hbar\omega + 2\mathcal{E}_F} \right] \text{grad}_{\parallel} |\vec{E}_{\parallel}|^2. \quad (16)$$

It is natural to relate both the photon energy $\hbar\omega$ and temperature T to the Fermi energy in order to obtain a more universal expression. Introducing the normalized quantities $s = \hbar\omega/\mathcal{E}_F$ and $\theta = k_B T/\mathcal{E}_F$, we find for the total ponderomotive force:

$$\vec{F}_{\text{tot}}^{(T>0)} = \overbrace{\frac{\hbar^2 e^2}{2m_{\text{eff}} \mathcal{E}_F^2} \text{grad}_{\parallel} |\vec{E}_{\parallel}|^2}^{=\vec{F}_1(s)} \cdot \underbrace{\frac{1}{s^2} \cdot \left[1 + \frac{s(s-2)}{(s-2)^2 + 4\theta^2} + \frac{s}{s+2} \right]}_{=P(s)}, \quad (17)$$

where the factor outside the bracket turns out to be the Drude-like intraband ponderomotive force \vec{F}_1 as indicated. The dimensionless function $P(s)$ summarizes the frequency-dependence and describes the ponderomotive force normalized to all appearing fundamental constants and the electric field gradient. In Fig. 1, we show $P(s)$ for a number of normalized temperatures θ .

V. NONLOCAL CORRECTIONS

For completeness, we finally present the main effect of nonlocality to the ponderomotive force at finite temperature. Since the ponderomotive force describes a nonlinearity, terms like “nonlocality” or “inhomogeneity” re-

quire clarification to avoid confusion. We consider the dependence of the ponderomotive force on the *optical* wave vector \vec{k}_{\parallel} projected to the sheet plane. In analogy to the scale separation in time mentioned in the preliminaries, we assume that the length scale of the charge distribution (i. e. the wavelength of the polariton) is large compared to \vec{k}_{\parallel} . It should be noted that this is not necessarily as good an assumption as the time-scale separation, because of the high confinement of the plasmon polaritons.

To the best of our knowledge, there is no model for the nonlocal effect in the intraband (Drude-like) conductance that is both applicable beyond the interband threshold ($s > 2$) and conducive for the style of analytical calculations we present in this paper. Therefore, we restrict ourselves to the effect of nonlocality on the interband case, which is anyway potentially of greater interest, because of its resonant nature.

The origin of the nonlocal interband effect is the conservation of momentum, where we assume a large graphene sheet and homogeneous optical illumination (spatially slowly varying envelope): A carrier from the lower branch of the dispersion relation with an initial wave vector on the circle $|\vec{q}_{\text{in}}| = q_0$ is not lifted to the same wave vector on the upper branch, but to a final wave vector on the circle that is shifted by the optical wave vector \vec{k}_{\parallel} : $|\vec{q}_{\text{fin}} - \vec{k}_{\parallel}| = q_0$. As a result, the effective interband transition energy is no longer independent of

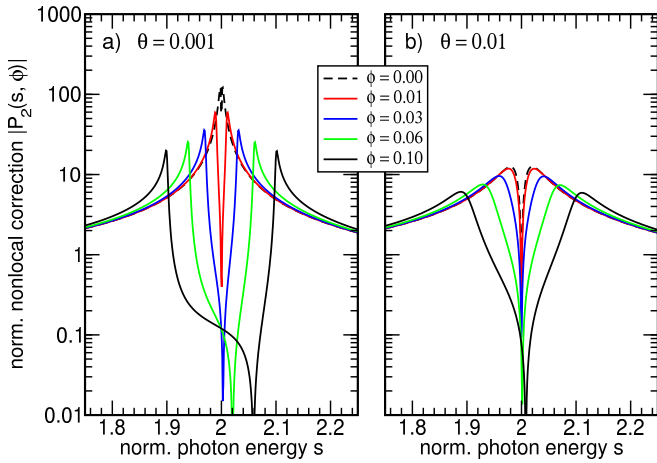


FIG. 2. Effect of nonlocality on the interband contribution to the ponderomotive force [Eq.(21)] at two normalized temperatures (panel a: $\theta = 0.001$; panel b: $\theta = 0.01$) and for several values of k_{\parallel} corresponding to different angles of incidence $\phi = k_{\parallel}/k_F$ of the driving light field.

the exact wave number on the initial wave number circle, but offset by up to $\pm v_F \vec{k}_{\parallel}$. Since all source states with the same energy form a circle in \vec{k} -space, we find for the nonlocally corrected conductance:

$$\sigma_2(\omega, k_{\parallel}) = \frac{1}{\pi} \int_{-\pi}^0 d\alpha \sigma_2(\omega + v_F k_{\parallel} \cos \alpha), \quad (18)$$

where the conductivity under the integral is the local conductivity and only the modulus k_{\parallel} of the optical wave vector matters because of the cylindrical symmetry of the Dirac cone. This smearing effect carries through the entire derivation and does not interact with the partial derivatives leading to the ponderomotive force. Hence, we find for the interband ponderomotive force including nonlocal corrections:

$$\vec{F}_2(\omega, k_{\parallel}) = \frac{1}{\pi} \int_{-1}^1 dz \frac{\vec{F}_2(\omega + v_F k_{\parallel} z)}{\sqrt{1 - z^2}}, \quad (19)$$

with $z = \cos \alpha$. We only study the seemingly more complex case of finite temperature, because at $T = 0$, there is a pole in the integration interval, which means that the zero temperature case must be obtained as the limit $T \rightarrow 0$ of the finite temperature expression. As before, we choose to separate the normalized frequency dependence from constants that clutter the notation by generalizing the inter-band contribution $P_2(s)$ to the normalized response function $P(s)$:

$$P_2(s, \phi) = \frac{1}{\pi} \int_{-1}^1 dz \frac{P_2(s + \phi z)}{\sqrt{1 - z^2}}, \quad (20)$$

where $\phi = k_{\parallel}/k_F$ is the normalized in-plane optical wave number and therefore simultaneously parameterizes the optical phase velocity and angle of incidence. As far as

we can tell, Eq. (20) has no closed solution in terms of fundamental functions, but under the assumptions $s \approx 2$ and $\phi \ll 1$ ($c \gg v_F$), we can approximate it (see Appendix A for details):

$$P_2(s, \phi) = 2I(s, \phi, -2) + I(s, \phi, 2 + 2i\theta) + I(s, \phi, 2 - 2i\theta) \quad (21a)$$

with

$$I(s, \phi, A) \approx \frac{(2s - A) \operatorname{sgn}(\Re\{s - A\})}{2s^2 \sqrt{(s - A)^2 - \phi^2}} - \frac{1}{2s^2}, \quad (21b)$$

where $\operatorname{sgn}(\Re\{z\}) = x/|x|$ for $z = x + iy$. We find that this approximate expression matches a direct numerical integration of Eq. (20) very well within in the range $1.5 \leq s \leq 2.5$ and $\phi \leq 0.1$, which corresponds to an optical wavenumber ten times higher than in vacuum.

In Fig. 2, we show Eq. (21) for two normalized temperatures and a number of normalized in-plane wave numbers. We find that the effect of the interband nonlocality on the ponderomotive force differs significantly from most nonlocal corrections found in plasmonics. Usually, nonlocality leads to spectral shifts as well as additional damping and smearing of spectral features e. g. due to Landau damping [35]. Instead, we find a splitting of the ponderomotive resonance in the regime $\phi > \theta$ corresponding to $k_{\parallel} > k_B T / \hbar v_F$. Below this threshold, the splitting exists in principle, but is hidden by thermal broadening.

VI. CONCLUSION

In summary, we derived an expression for the ponderomotive force arising from the optical excitation of a polariton in a 2D material, focusing our analysis on the case of graphene. Starting from a thermodynamic approach that relates the material permittivity to the total free enthalpy, we obtained a general relation between the ponderomotive force and the 2D sheet conductivity. By introducing into this the appropriate expression for the interband graphene conductivity, we showed that the resulting ponderomotive force exhibits a pole, which leads to its divergence at zero temperature. At higher temperatures, this divergence is gradually smoothed, but there is always an energy region around half the Fermi energy where the interband contribution is larger than the corresponding Drude part. This can play an important role when exploring second-order intrinsic nonlinearities in polaritonic materials, as for example in the recent study of stimulated plasmon polariton scattering [36]. Finally, we explored the impact of nonlocal corrections to the interband part assuming a spatially slowly varying optical envelope, and found a very characteristic type of resonance splitting. Strikingly, this is very distinct from the simple broadening and minuscule resonance shifts, which are the most common type of nonlocal correction in linear plasmonics [37–39], and therefore a very clear signature for nonlocal response in plasmonics.

ACKNOWLEDGMENTS

C. W. acknowledges funding from a MULTIPLY fellowship under the Marie Skłodowska-Curie COFUND Action (grant agreement No. 713694). The Center for Nano Optics is financially supported by the University of Southern Denmark (SDU 2020 funding). C. W. also acknowledges controversial yet fruitful discussions with

Dr Wolff. N. A. M. is a VILLUM Investigator supported by VILLUM Fonden (grant No. 16498). The Center for Nanostructured Graphene is sponsored by the Danish National Research Foundation (Project No. DNRF103).

Appendix A: Analytic approximation to the nonlocal correction

Here, we find an approximate solution to the integral

$$P_2(s, \phi) = \frac{1}{\pi} \int_{-1}^1 dz \frac{1}{\sqrt{1-z^2}} \frac{1}{s+\phi z} \left[\frac{s+\phi z-2}{(s+\phi z-2)^2+4\theta^2} + \frac{1}{s+\phi z+2} \right] \quad (\text{A1})$$

$$= \frac{1}{2\pi} \int_{-1}^1 dz \frac{1}{\sqrt{1-z^2}} \cdot \frac{1}{s+\phi z} \left[\frac{1}{s+\phi z-2+2i\theta} + \frac{1}{s+\phi z-2-2i\theta} + \frac{2}{s+\phi z+2} \right]. \quad (\text{A2})$$

This partial fraction decomposition reduces the problem to three integrals of the same form

$$I(s, \phi, A) = \frac{1}{2\pi} \int_{-1}^1 dz \frac{1}{\sqrt{1-z^2}} \cdot \frac{1}{s+\phi z} \cdot \frac{1}{s+\phi z-A}. \quad (\text{A3})$$

Next, we restrict ourselves to the neighborhood of the inter-band resonance, i. e. $s \approx 2$ and we assume $\phi \ll 1$. This means we may approximate $(s+\phi z)^{-1} \approx s^{-2}(s-\phi z)$:

$$I(s, \phi, A) \approx \frac{1}{2\pi s^2} \int_{-1}^1 dz \frac{1}{\sqrt{1-z^2}} \cdot \frac{s-\phi z}{\phi z+s-A} = \frac{1}{2\pi s^2} \int_{-1}^1 dz \frac{1}{\sqrt{1-z^2}} \left[\frac{2s-A}{\phi z+s-A} - 1 \right] \quad (\text{A4})$$

$$= \frac{-1}{2s^2} + \frac{2s-A}{2\pi\phi s^2} \int_{-1}^1 dz \frac{1}{(z+a)\sqrt{1-z^2}}, \quad \text{with } a = \frac{s-A}{\phi}. \quad (\text{A5})$$

This is a standard integral and evaluates to $\pi/\sqrt{a^2-1}$. This expression is ambiguous as to which branch of the root function is to be used. This is solved by identifying the integration result at $\phi = 0$ with the local expression $P_2(s)$. In this way, we arrive at Eq. (21).

-
- [1] A. H. Castro Neto, F. Guinea, N. M. R. Peres, K. S. Novoselov, and A. K. Geim, *Rev. Mod. Phys.* **81**, 109 (2009).
 - [2] A. C. Ferrari, F. Bonaccorso, V. Fal'ko, K. S. Novoselov, S. Roche, P. Bøggild, S. Borini, F. H. L. Koppens, V. Palermo, N. Pugno, J. A. Garrido, R. Sordan, A. Bianco, L. Ballerini, M. Prato, E. Lidorikis, J. Kivioja, C. Marinelli, T. Ryhnen, A. Morpurgo, J. N. Coleman, V. Nicolosi, L. Colombo, A. Fert, M. Garcia-Hernandez, A. Bachtold, G. F. Schneider, F. Guinea, C. Dekker, M. Barbone, Z. Sun, C. Galiotis, A. N. Grigorenko, G. Konstantatos, A. Kis, M. Katsnelson, L. Vandersypen, A. Loiseau, V. Morandi, D. Neumaier, E. Treossi, V. Pellegrini, M. Polini, A. Tredicucci, G. M. Williams, B. H. Hong, J.-H. Ahn, J. M. Kim, H. Zirath, B. J. van Wees, H. van der Zant, L. Occhipinti, A. Di Matteo, I. A. Kinloch, T. Seyller, E. Quesnel, X. Feng, K. Teo, N. Rupesinghe, P. Hakonen, S. R. T. Neil, Q. Tannock, T. Löfwander, and J. Kinaret, *Nanoscale* **7**, 4598 (2015).
 - [3] M. Xu, T. Liang, M. Shi, and H. Chen, *Chem. Rev.* **113**, 3766 (2013).
 - [4] S. Z. Butler, S. M. Hollen, L. Cao, Y. Cui, J. A. Gupta, H. R. Gutiérrez, T. F. Heinz, S. S. Hong, J. Huang, A. F. Ismach, E. Johnston-Halperin, M. Kuno, V. V. Plashnitsa, R. D. Robinson, R. S. Ruoff, S. Salahuddin, J. Shan, L. Shi, M. G. Spencer, M. Terrones, W. Windl, and J. E. Goldberger, *ACS Nano* **7**, 2898 (2013).
 - [5] I. W. Frank, D. M. Tanenbaum, A. M. van der Zande, and P. L. McEuen, *J. Vac. Sci. Technol. B* **25**, 2558 (2007).
 - [6] A. A. Balandin, *Nat. Nanotechnol.* **10**, 569 (2011).
 - [7] G. Fiori, F. Bonaccorso, G. Iannaccone, T. Palacios, D. Neumaier, A. Seabaugh, S. K. Banerjee, and L. Colombo, *Nat. Nanotechnol.* **9**, 768 (2014).
 - [8] F. Xia, H. Wang, D. Xiao, M. Dubey, and A. Ramasubramanian, *Nat. Photon.* **8**, 899 (2014).
 - [9] D. L. Mills and E. Burstein, *Rep. Prog. Phys.* **37**, 817 (1974).

- [10] A. V. Zayats and I. I. Smolyaninov, *J. Opt. A: Pure Appl. Opt.* **5**, S16 (2003).
- [11] P. A. D. Gonçalves and N. M. R. Peres, *An Introduction to Graphene Plasmonics* (World Scientific, Singapore, 2016).
- [12] S. Xiao, X. Zhu, B.-H. Li, and N. A. Mortensen, *Front. Phys.* **11**, 117801 (2016).
- [13] T. Low, A. Chaves, J. D. Caldwell, A. Kumar, N. X. Fang, P. Avouris, T. F. Heinz, F. Guinea, L. Martín-Moreno, and F. Koppens, *Nat. Mater.* **16**, 182 (2017).
- [14] E. Hendry, P. J. Hale, J. Moger, A. K. Savchenko, and S. A. Mikhailov, *Phys. Rev. Lett.* **105**, 097401 (2010).
- [15] M. Gullans, D. E. Chang, F. H. L. Koppens, F. J. García de Abajo, and M. D. Lukin, *Phys. Rev. Lett.* **111**, 247401 (2013).
- [16] A. R. Echarri, J. D. Cox, R. Yu, and F. J. García de Abajo, *ACS Photonics* **5**, 1521 (2018).
- [17] J. L. Cheng, J. E. Sipe, N. Vermeulen, and C. Guo, *J. Phys.: Photonics* **1**, 015002 (2018).
- [18] J. W. You, S. R. Bongu, Q. Bao, and N. C. Panoui, *Nanophotonics* **8**, 63 (2019).
- [19] R. W. Boyd, *Nonlinear optics, 3rd edition* (Academic Press, 2003).
- [20] L. D. Landau, E. M. Lifshitz, and L. P. Pitaevskii, *Electrodynamics of continuous media; 2nd ed.*, Course of theoretical physics (Butterworth, Oxford, 1984).
- [21] G. Malka and J. L. Miquel, *Phys. Rev. Lett.* **77**, 75 (1996).
- [22] S. Leinß, T. Kampfath, K. von Volkman, M. Wolf, J. T. Steiner, M. Kira, S. W. Koch, A. Leitenstorfer, and R. Huber, *Phys. Rev. Lett.* **101**, 246401 (2008).
- [23] S. D. Irvine, P. Dombi, G. Farkas, and A. Y. Elezzabi, *Phys. Rev. Lett.* **97**, 146801 (2006).
- [24] K. Johnsen and A.-P. Jauho, *Phys. Rev. Lett.* **83**, 1207 (1999).
- [25] P. Ginzburg, A. Hayat, N. Berkovitch, and M. Orenstein, *Opt. Lett.* **35**, 1551 (2010).
- [26] S. A. Mikhailov, *Phys. Rev. B* **84**, 045432 (2011).
- [27] S.-Y. Hong, J. I. Dadap, N. Petrone, P.-C. Yeh, J. Hone, and R. M. Osgood Jr., *Phys. Rev. X* **3**, 021014 (2013).
- [28] J. L. Cheng, N. Vermeulen, and J. E. Sipe, *Opt. Express* **22**, 15868 (2014).
- [29] Z. Sun, D. N. Basov, and M. M. Fogler, *Proc. Natl. Acad. Sci. U. S. A.* **115**, 3285 (2018).
- [30] T. Stauber, N. M. R. Peres, and A. K. Geim, *Phys. Rev. B* **78**, 085432 (2008).
- [31] Y.-C. Chang, C.-H. Liu, C.-H. Liu, S. Zhang, S. R. Marder, E. E. Narimanov, Z. Zhong, and T. B. Norris, *Nat. Commun.* **7**, 10568 (2016).
- [32] Strictly speaking, our thermodynamic potential $\tilde{\mathcal{G}}$ is not the free enthalpy, which is defined with the electric induction \vec{D} as the independent variable and connected to $\tilde{\mathcal{G}}$ via a Legendre transformation [20]. This detail is of no concern for our argument.
- [33] N. M. R. Peres, Y. V. Bludov, J. E. Santos, A. P. Jauho, and M. I. Vasilevskiy, *Phys. Rev. B* **90**, 125425 (2014).
- [34] X. Yao, M. Tokman, and A. Belyanin, *Phys. Rev. Lett.* **112**, 055501 (2014).
- [35] S. Raza, S. I. Bozhevolnyi, M. Wubs, and N. A. Mortensen, *J. Phys.: Condens. Matter* **27**, 183204 (2015).
- [36] C. Wolff and N. A. Mortensen, arXiv:1812.05826 .
- [37] S. Raza, S. Kadkhodazadeh, T. Christensen, M. Di Vece, M. Wubs, N. A. Mortensen, and N. Stenger, *Nat. Commun.* **6**, 8788 (2015).
- [38] T. Christensen, W. Wang, A.-P. Jauho, M. Wubs, and N. A. Mortensen, *Phys. Rev. B* **90**, 241414(R) (2014).
- [39] T. Christensen, W. Yan, A.-P. Jauho, M. Soljačić, and N. A. Mortensen, *Phys. Rev. Lett.* **118**, 157402 (2017).